Stability Analysis of Horizontal and Vertical Paste Fill Exposures at the Raleigh Mine

Sainsbury, D. P.
Itasca Australia Pty Ltd, Melbourne, Victoria, Australia
Urie, R.
Barrick - Kanowna, Kalgoorlie, Western Australia, Australia

ABSTRACT: The uphole bench extraction strategy at EKJV Management Pty Ltd's Raleigh Mine, requires simultaneous horizontal and vertical exposure of paste filled stopes. In order to prevent excessive ore dilution, the paste fill must be of sufficient strength to prevent failure during exposure. A numerical modelling methodology has been developed to accurately simulate the initial stress distribution within paste filled stopes, together with the strain-softening loading response of paste fill material. Due to the narrow orebody width and high deformation behaviour of the host rock mass, high closure strains are likely to cause a stiff, brittle fill material to undergo crushing failure upon exposure.
The stability of paste fill exposures at the Raleigh Mine was determined by conducting a series of three-dimensional numerical models that incorporate the extraction, filling and exposure sequence of paste filled stopes. Stability charts for 2.5 m and 3.5 m wide simultaneous horizontal and vertical exposures have been derived based upon the numerical modelling results. Implementation of the stability charts has proved successful in limiting the amount of ore dilution from paste fill and provides a basis to optimize paste fill cementation and stability throughout the life of the mine.

1. INTRODUCTION

The uphole bench extraction strategy at the Raleigh Mine requires simultaneous horizontal and vertical exposure of narrow (2.5 – 3.5 m) paste filled stopes. Due to the narrow exposure span, high closure strain caused by deformation of the adjacent rock mass is likely to cause a stiff, brittle fill material to undergo crushing failure. Three-dimensional numerical modelling has been conducted with the FLAC3D code to engineer a fill material of low modulus to prevent crushing failure when subjected to high closure strain, but of sufficient strength to prevent caving failure.

2. MINING GEOMETRY

The uphole bench stoping extraction strategy at the Raleigh Mine is illustrated in Figure 1. Each stope consists of three offset panels, which are retreated back to connect with the panel above. Paste fill is then placed from the upper ore drive, which cascades through the upper two panels to initially fill the lower panel then the middle panel and finally the upper panel.

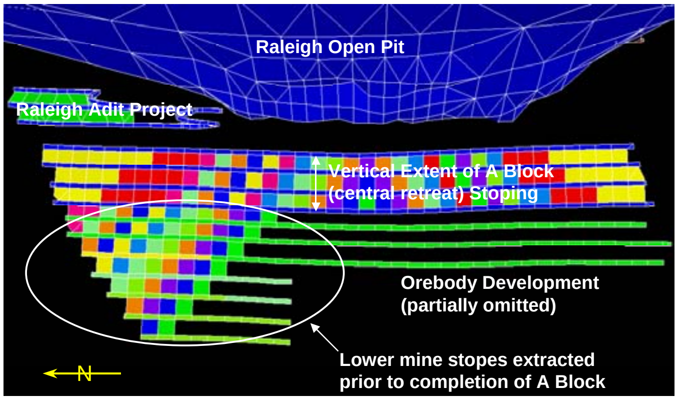

Fig. 1.Raleigh Mine extraction strategy.

The orebody is typically 0.5 m thick and dips at approximately 63^{o}. The ore is accessed by means of ore drive sub-levels at 16.5 m vertical intervals. The benches are established at a width of approximately 2.5 – 3.5 m and a strike length of 15 m.

The paste filled benches are exposed simultaneously along horizontal and vertical faces due to the angled benching front. Due to the rapid mining cycle, paste fill is exposed after a curing time of four days.

Figure 2 illustrates a vertical paste fill exposure at the Raleigh Mine. To date, only minor paste fill dilution has been observed after blasting. This dilution is caused by blast-induced damage.

Fig. 2. Vertical paste fill exposure at the Raleigh Mine.

3. GEOMECHANICAL LABORATORY TESTING OF RALEIGH PASTE FILL

A detailed laboratory testing program has been conducted to determine the geomechanical properties of Raleigh paste fill.

3.1. Unconfined Compressive Strength

Unconfined compressive strength (UCS) testing was conducted to investigate the effects of curing time, cement content, slump (solids content) tailings/sand ratio and binder content. The UCS of Raleigh paste fill with 6%$_{wt}$ cement, 210-230mm slump and a tailings to sand ratio of 70:30 (Mix 1) is illustrated in Figure 3. A clear increase in strength is achieved with increasing cure time. As observed, the UCS of the paste fill is extremely sensitive to the solids content, or slump, of the paste mixture. To help estimate the ultimate strength of Raleigh paste, the results of the early-age UCS tests have been compared to the UCS results of similar paste fill materials as illustrated in Figure 4 (the low solids content (75%) is responsible for the low strength of the Golden Giant paste). It can be expected that Raleigh paste will continue to gain strength up to 56 days curing time.

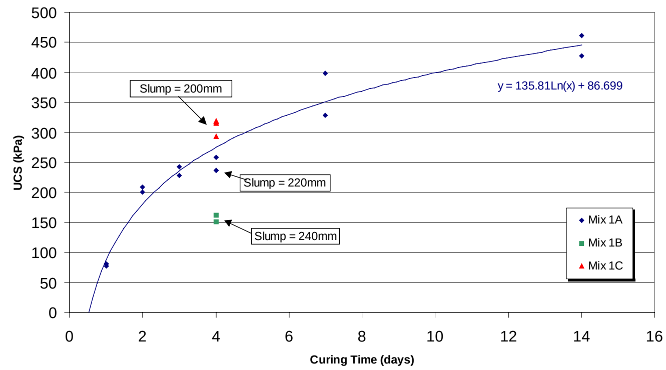

Fig. 3. UCS results of early-age Raleigh paste with 6%$_{wt}$ cement, 210-230mm slump, 70:30 tailings:sand.

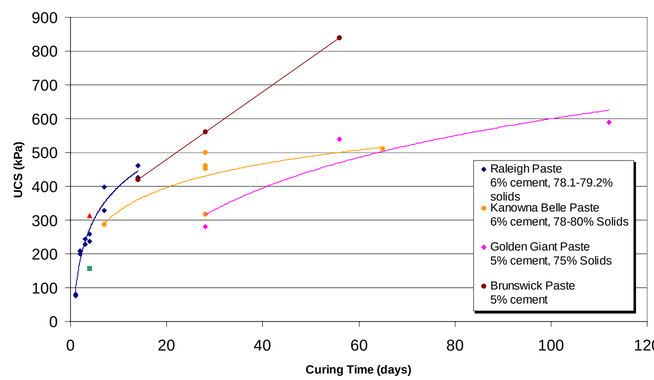

Fig. 4. UCS results of early-age Raleigh paste with 6%$_{wt}$ cement, 210-230mm slump, 70:30 tailings:sand together with similar paste fill UCS results [Kanowna Belle paste results (Sainsbury and Pierce, 2005); Golden Giant paste results (Pierce, 1997); Brunswick paste results (Pierce, 2000)].

3.2. Young's Modulus

The Young's Modulus was determined from the stress-strain curve of a limited number of the UCS tests. Figure 5 illustrates the relation between Young's Modulus and UCS for Mix 1 Raleigh paste, together with Young's Modulus for other similar paste fill materials. It is believed that the low Young's Modulus values are related to the early age of the paste fill. The values obtained for other paste fill materials are from UCS tests conducted at curing times of 28 and 56 days. Generally, as the strength of the paste increases, so does the Young's modulus.

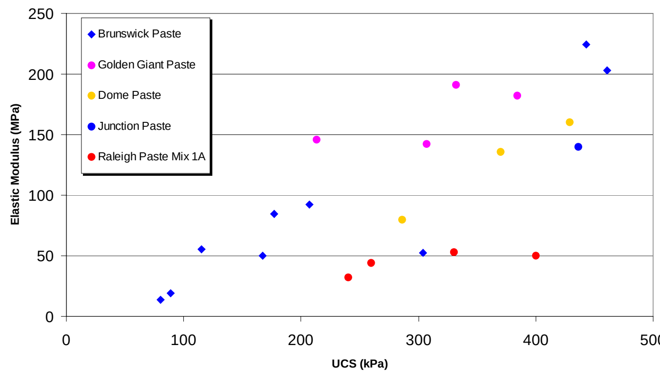

Fig. 5. Relation between Young's modulus and UCS of Raleigh paste together similar paste-fill materials [Kanowna Belle paste results (Sainsbury and Pierce, 2005); Golden Giant paste results (Pierce, 1997); Brunswick paste results (Pierce, 2000); Junction paste results (Sainsbury, 2003); Dome paste results (Aref et al., 1989)]

3.3. *Tensile Strength*

Tensile strength is an important parameter when assessing the stability of horizontal (underhand) paste fill exposures. Two separate testing methods were employed to determine the tensile strength of Mix 1 Raleigh paste after 4 days curing time: the Brazilian test and the three-point bending (Flexure) test. The Brazilian test is used to determine the tensile strength of intact rock. Generally, the test is not appropriate for paste fill, as the material must be brittle for the test to be valid (Fairhurst, 1964). Neville (1963) suggests that the most appropriate method for determining the tensile strength of concrete is the three-point bending test.

Mitchell and Wong (1982) conducted a series of tensile strength tests on cemented tailings sands using both the three-point bending method and direct tension testing. Tensile strengths from both tests gave similar results; the average tensile strength was found to be 12% of the unconfined compressive strength. Figure 6 illustrates the results of the tensile strength results of Raleigh paste compared to the tensile strength of similar paste fill material obtained from a variety of testing methods. The results of the two three-point bending tests conducted on Mix 1 Raleigh paste after 4 days of curing time appear abnormally high. The results of the Brazilian tests are more consistent with the relation between tensile strength and UCS for other similar paste-fill materials. Mitchell and Wong's 12% of the UCS rule-of-thumb provides a reasonable estimate of the tensile strength of different paste fill materials.

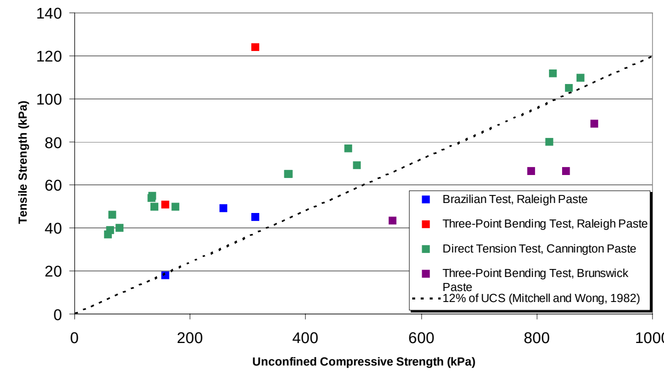

Fig. 6. Tensile strength results compared to similar paste fill material [Brunswick paste results (Pierce, 2000); Cannington paste results (Rankine et al., 2001)]

3.4. *Triaxial Shear Strength*

The shear strength of backfill is required for assessing stability during both vertical and horizontal exposure. Two consolidated-undrained (CU) triaxial compression tests were conducted to determine the effective shear strength parameters of Mix 1 Raleigh paste after 4 days curing time.

The effective strength envelope derived from the CU test is illustrated in Figure 7. The effective shear-strength parameters *c'* and ϕ' were obtained from the undrained test results by subtracting the pore pressures at failure from the total stresses at failure. The *c'* and ϕ' values obtained were 70 kPa and 40°, respectively. The equivalent UCS is calculated as 300 kPa. This is consistent with the UCS tests conducted on the same Mix 1 material (313 kPa).

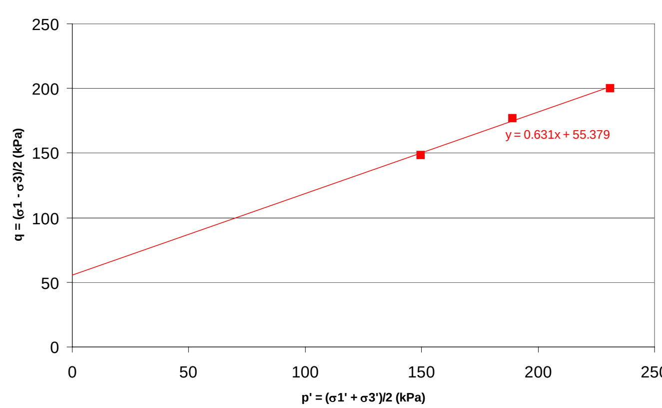

Fig. 7. Effective strength envelope of Mix 1 Raleigh paste after 4 days curing time.

The friction angle obtained from similar paste fill mixtures are illustrated in Figure 8. Compared to other similar paste materials, the friction angle of

Raleigh paste is slightly high, although only a single value has been obtained for comparison.

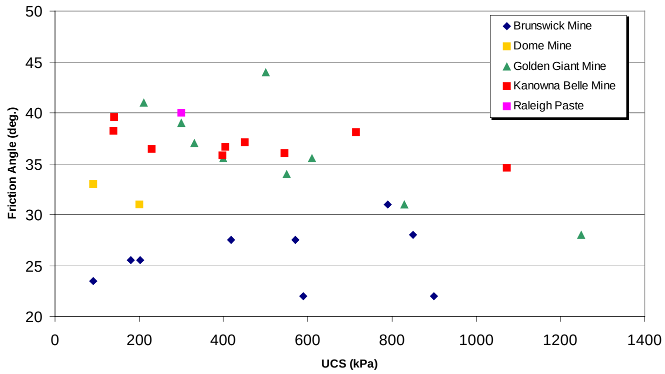

Fig. 8. Friction angle versus unconfined compressive strength for paste fill samples from different operations [Golden Giant paste results (Pierce, 1997); Brunswick paste results (Pierce, 2000); Dome paste results (Aref et al., 1989)]

4. NUMERICAL MODELLING OF PASTE FILL EXPOSURES

Due to the fine-grained, homogeneous nature of paste fill, the three-dimensional numerical modeling code FLAC3D (Itasca, 2005) was used to model the stability of simultaneous horizontal and vertical paste fill exposures.

4.1. Model Geometry

The model geometry used to simulate the Raleigh uphole bench extraction sequence is illustrated in Figure 9. The extraction sequence is simulated by excavating and filling panels over three sub-levels. After filling, the horizontal and vertical exposure of the middle bench is monitored for stability during retreat of the adjacent benches in four excavation stages.

4.2. Modelling Methodology

The results of triaxial testing of paste fill indicate that, over the range of confining stresses expected *in situ*, the shear strength can be represented by a straight line on a plot of shear stress vs normal stress. Therefore, the shear strength can be modelled adequately by cohesion and a friction angle (Mohr-Coulomb constitutive model). With such a model, the paste fill is assumed to behave elastically at stress states below its shear strength. Once the fill reaches its peak shear strength, shear yielding occurs, and the fill can undergo large-scale plastic deformations.

Modelling of paste fill behaviour has been conducted using the effective shear-strength parameters to simulate the shear strength of the paste fill. It was further assumed that positive pore pressures are not developed *in situ* as a result of load changes accompanying fill exposure. An *in situ* monitoring program is currently being conducted at the Raleigh Mine to provide greater understanding of *in situ* behaviour of Raleigh paste. Initial monitoring results indicate that negative pore pressures develop within the fill mass approximately 27 hours after placement.

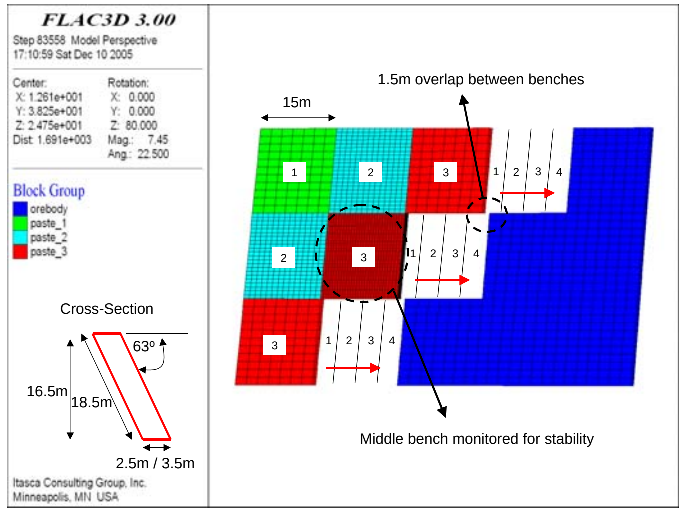

Fig. 9. Model geometry used to investigate 2.5 m exposure width (surrounding rock mass hidden).

4.3. Strain Softening

The stress-strain response of different strength paste fill materials in unconfined compression is illustrated in Figure 10. Inspection of the different curves shows that for low-strength paste fill, the shear strength remains constant once yielding begins (ductile or perfectly plastic response). This differs from higher-strength paste fill that loses some or all of the cohesion upon yielding (brittle or strain-softening response).

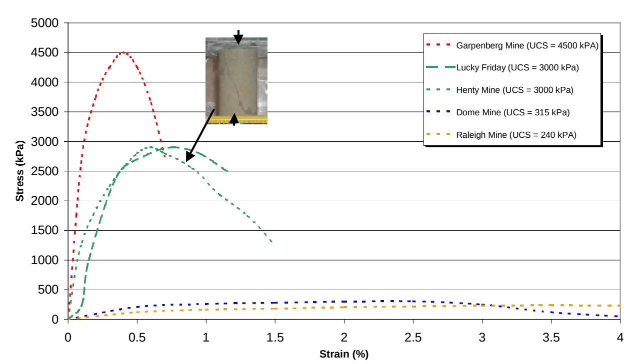

Fig. 10. Stress-strain response of different strength paste fill materials in uniaxial compression.

The specification of ductile or brittle behaviour in a numerical model is a very important consideration, as brittle materials tend to undergo progressive collapse much sooner after yielding begins. Ductile materials, on the other hand, are likely to remain stable well after yielding begins. For this reason, a Mohr-Coulomb strain-softening model has been used to represent the post-peak strength degradation of the paste fill upon loading. In order to simulate the strain-softening behaviour of paste fill, the decrease in strength as a function of the plastic strain (εps) accumulated in the yielding material needs to be described explicitly. To simulate a strain softening response in a Mohr-Coulomb material, the cohesion and tensile strength can be decreased linearly from their maximum value at zero plastic strain, down to zero at a critical plastic strain (εps_{crit}) value. Depending upon the stress-path imposed, a strain softening material will exhibit shear bands, in which the shear strain is localized, rather than being uniformly distributed.

Swan and Brummer (2001) and later Pakalnis et al., (2005) have specified a critical plastic strain (εps_{crit}) value of 1.5% to represent the softening response of paste fill in FLAC and FLAC3D, irrespective of the zone size, aspect ratio or resolution of the model. However, when using a strain softening constitutive model, it must be understood that the stress - strain relation generated is strongly grid dependant. This is because the strain concentrated in a localized shear band depends on the width of the band (in length units), which depends on zone size. Hence smaller zones lead to more softening.

Figure 11 illustrates the UCS stress – strain response of two models, one with a zone size of 3.75 mm and another with a zone size of 7.5 mm. The same critical plastic strain (εps_{crit}) value was used to degrade the cohesion and tensile strength from their maximum value to. Clearly, the global softening response is greater in the finer zoned model.

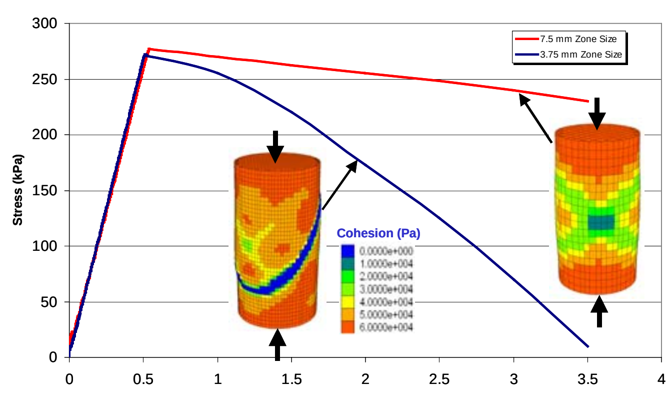

Fig. 11. Softening response of coarse and fine UCS models.

To correct this grid dependence, a calibration exercise must be conducted to match the global response of different laboratory tests. Figure 12 illustrates the calibrated response of a series of paste unconfined and triaxial strength test results. Once the strain softening response has been calibrated for a particular zone size, the critical plastic strain (εps_{crit}) can be scaled for paste exposure scale models with larger zone sizes.

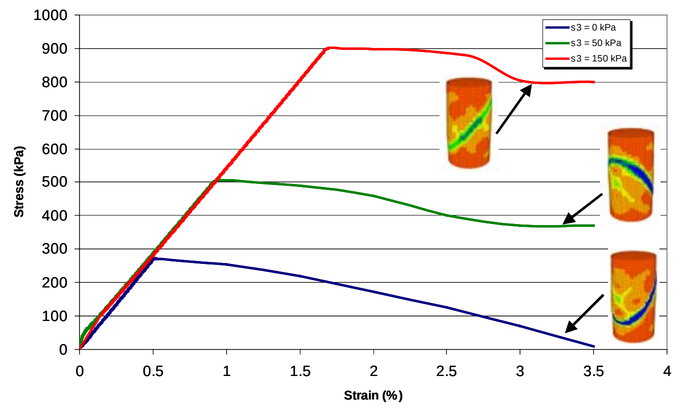

Fig. 12. Calibrated stress – strain response of UCS and triaxial strength test results.

For this study, the critical plastic strain (εps_{crit}) was calibrated to the UCS stress-strain response of different strength paste materials, as illustrated in Figure 13. A relation between critical plastic strain (εps_{crit}) and UCS was derived to simulate the increasing "brittleness" with an increase in strength.

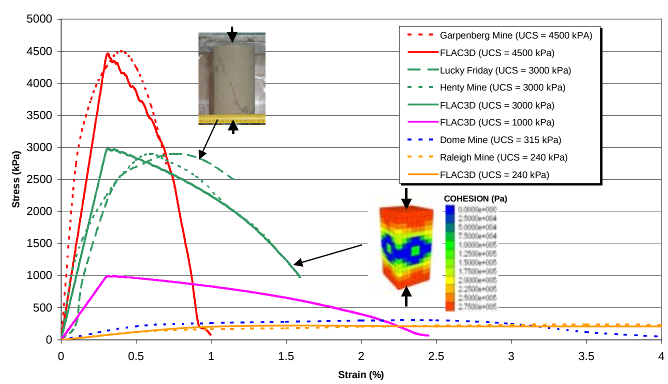

Fig. 13. Stress-strain response of different strength paste fill materials compared to simulated FLAC3D UCS tests.

4.4. *Initial Stress Distribution within a Fill Mass*

Vertical stresses in fill often are lower than their theoretical dead-weight values due to the arching of stresses into the stope walls. The amount of stress arching increases with fill friction angle and decreases with an increase in stope width. If arching is not taken into account, initial stresses can be overestimated, especially near the base of high stopes.

The stope-filling process was modelled explicitly within FLAC3D by initializing sequential lifts of fill until the excavated stope is filled. As the sequential lifts of fill are added, the effects of fill arching are accounted for by the modelling process, which allows stresses to arch into the rigid walls of the stope.

4.5. Behaviour of Fill-Rock Interfaces

The behavior of fill-rock interfaces is a function of the large-scale roughness of the stope wall rock. The stope walls in the modelling exercise were assumed to be sufficiently rough that shear failure at a fill-rock interface will involve shearing through the fill, rather than along the fill-rock interface itself. As a result, it is assumed in the model that these interfaces have the same shear strength as the fill (i.e., both a cohesion and a friction angle are specified). The tensile strengths of fill-fill and fill-rock interfaces are assumed to be zero, as little bonding is expected to occur across the interface itself.

4.6. Rock Mass Response to Mining

The host rock mass and representative pre-mining stresses are included in the model to account for the rock mass response to mining. In order to simulate a range of hangingwall/footwall convergences, the rock mass deformation modulus was varied from 3 GPa to 200 GPa.

Figure 14 illustrates the total hangingwall displacement, along with the convergence across the center of the middle filled bench, caused by retreat of the adjacent bench in four excavation stages. This level of convergence is representative of a rock mass deformation modulus of 50 GPa.

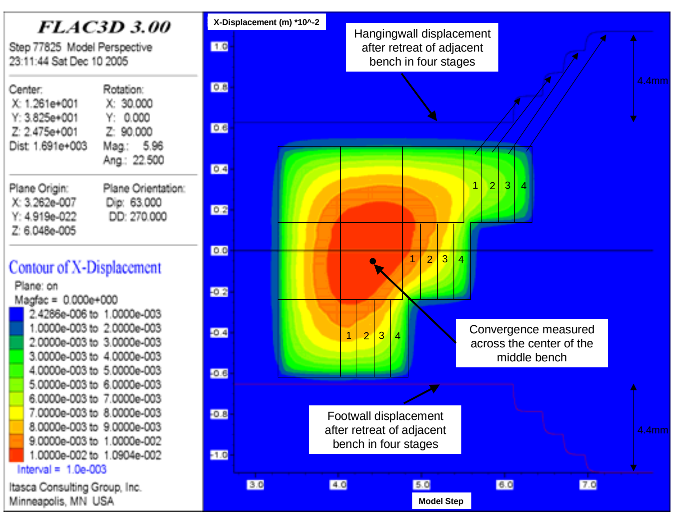

Fig. 14. Total hangingwall displacement and convergence after retreat of adjacent bench in four excavation stages.

5. MODEL RESULTS

A series of analyses were conducted to investigate the stability of 2.5 m wide paste exposures developed within the Raleigh extraction sequence. Depending upon the strength of the paste fill and the hangingwall/footwall convergence, different failure mechanisms were observed. Five separate stability classifications have been defined based upon the numerical modelling results. They include: caving failure, no yielding, minor yielding, significant yielding and crushing failure.

An example of the caving failure classification is illustrated in Figure 15. For paste fill UCS strengths less than 70 kPa at low levels of convergence, yielding of the horizontal exposure is controlled by the tensile strength of the paste fill. Complete degradation of the paste fill is predicted to extend 3 – 5 m from the horizontal exposure. Only minor yielding of the vertical exposure is predicted.

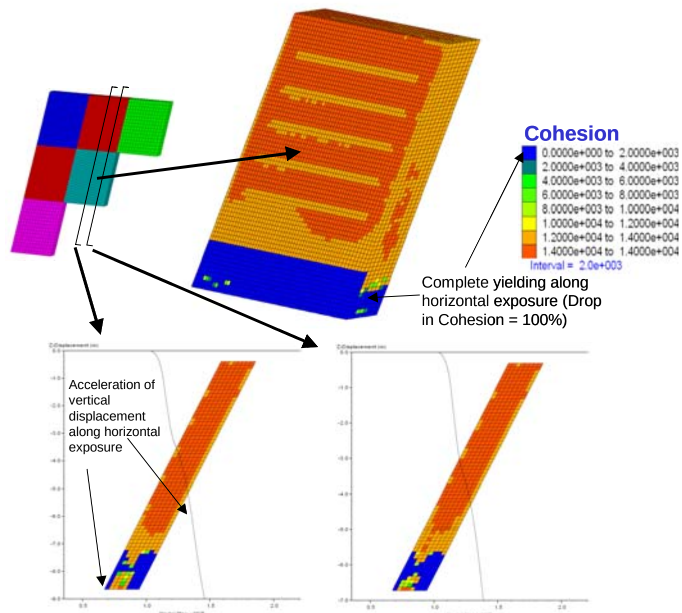

Fig. 15. Caving failure classification.

An example of the no-yielding classification is illustrated in Figure 16. For paste fill UCS strengths greater than 70 kPa at low levels of convergence, no yielding of the horizontal or vertical exposure is predicted.

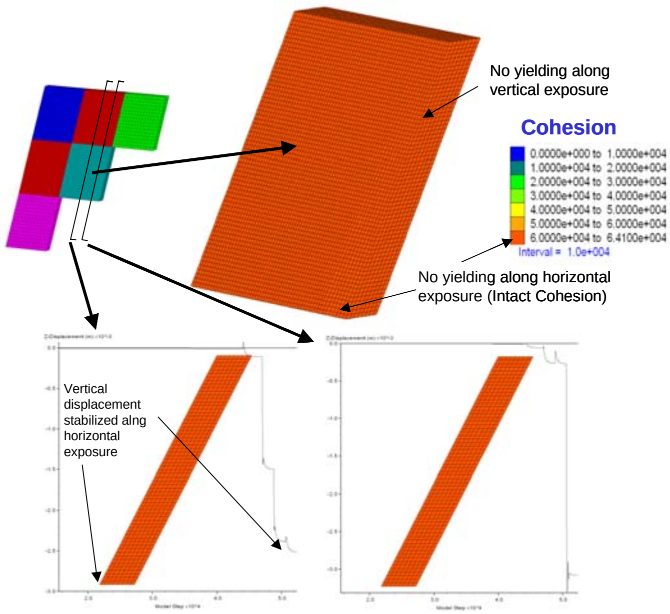

Fig. 16. No-yielding classification.

An example of the minor yielding classification is illustrated in Figure 17. For paste fill UCS strengths greater than 70 kPa at minor levels of convergence, minor yielding of the horizontal exposure is controlled by the shear strength of the paste fill. Minor degradation of the paste strength is predicted at the intersection of the horizontal and vertical exposure. Only minor yielding of the vertical exposure is predicted.

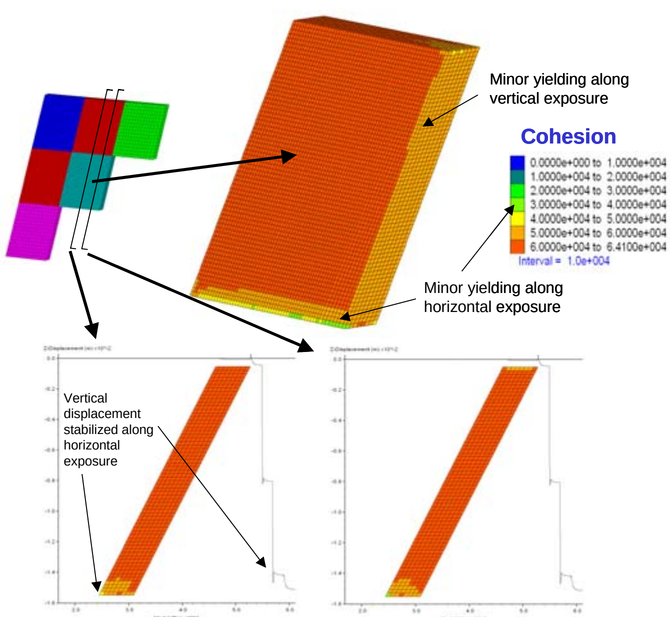

Fig. 17. Minor-yielding classification.

An example of the significant-yielding classification is illustrated in Figure 18. For paste fill UCS strengths greater than 70 kPa at moderate levels of convergence, complete degradation of the paste strength is predicted at the intersection of the horizontal and vertical exposure. Only minor yielding of the vertical exposure is predicted.

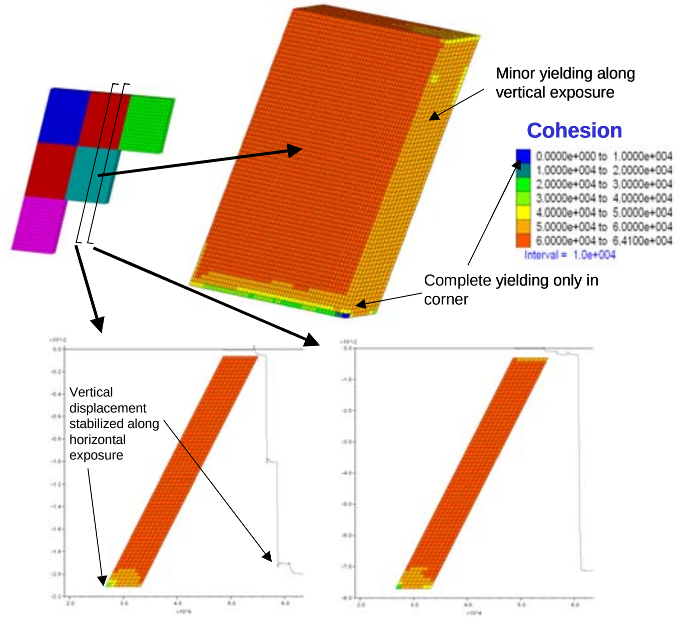

Fig. 18. Significant-yielding classification.

An example of the crushing-failure classification is illustrated in Figure 19. For paste fill UCS strengths greater than 70 kPa at high levels of convergence, complete degradation of the paste strength is predicted to extend 3 – 5 m from the horizontal exposure. Significant yielding of the vertical exposure is predicted.

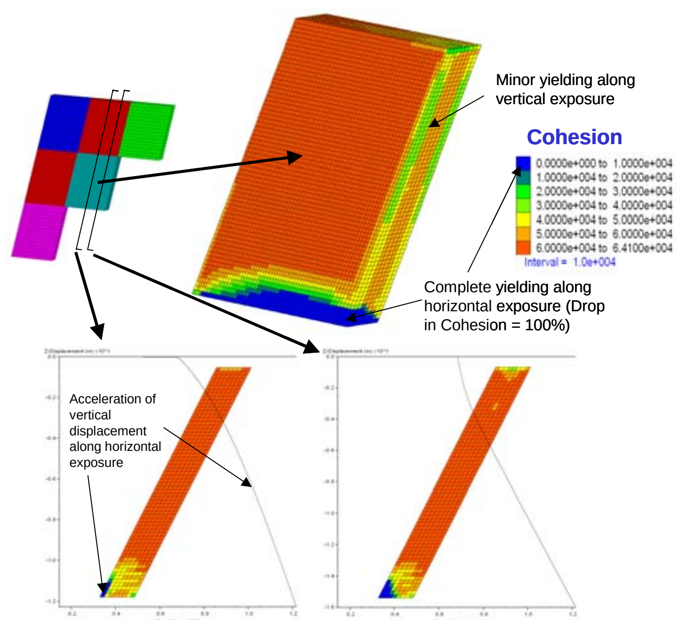

Fig. 19. Crushing-failure classification.

The results of the numerical analyses for 2.5 m wide simultaneous horizontal and vertical exposures have been summarised in a stability chart presented in Figure 20.

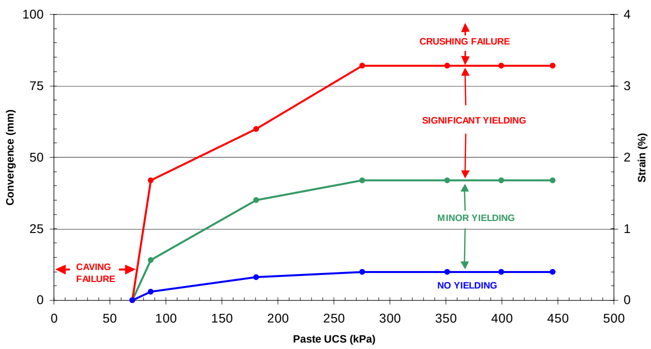

Fig. 20. Stability Chart for 2.5 m wide simultaneous horizontal and vertical exposures.

In order to test the sensitivity of stability to the exposure width, a series of analyses were conducted with a 3.5 m exposure width. The same stability classifications were observed to apply to the wider exposures. However, due to the increased width, caving failure was predicted at fill UCS strengths less that 115 kPa. The results of the numerical analyses have been summarised in a stability chart presented in Figure 21.

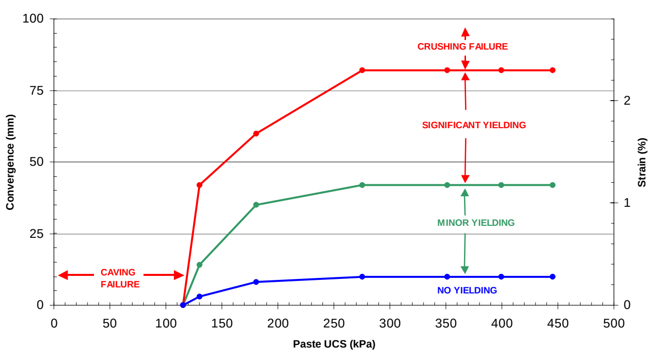

Fig. 21. Stability Chart for 3.5 m wide simultaneous horizontal and vertical exposures.

6. DISCUSSION OF RESULTS

For 2.5 and 3.5 m wide simultaneous horizontal and vertical paste fill exposures, an increase in paste fill UCS beyond 275 kPa does not translate to an increase in stability. This phenomenon is caused by the increase in modulus and "brittleness" with increasing paste fill strength.

The stability condition for 275 kPa strength paste fill with increasing convergence is illustrated in Figure 22. Preliminary linear elastic modeling indicates that the expected convergence upon exposure will be approximately 21 mm. As illustrated, for a convergence of 21 mm, a paste UCS of 250 kPa will experience minor yielding. This level of yielding is likely to manifest as less than 0.5 m overbreak along the hangingwall haunch at the intersection of the horizontal and vertical exposures. This classification is consistent with the observation of paste fill exposure performance during the early stages of extraction at the Raleigh Mine.

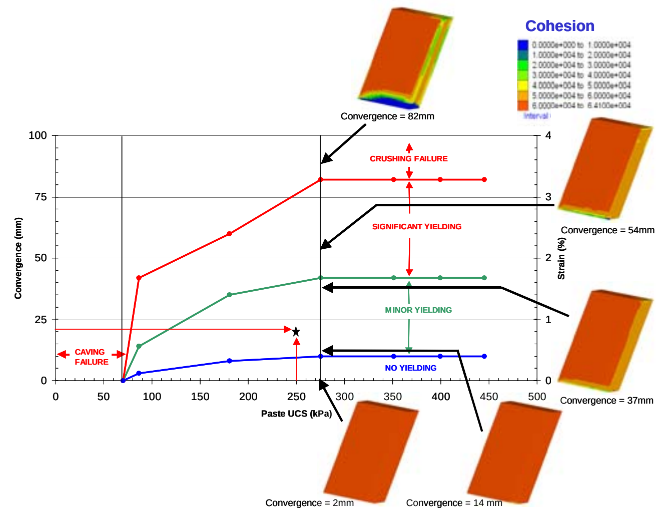

Fig. 22. Stability condition of 250 kPa strength paste fill for a 2.5 m wide simultaneous vertical and horizontal exposures.

The calibrated design charts are currently being used to optimize the degree of cementation required to achieve fill stability during exposure at the Raleigh Mine.

7. CONCLUSIONS

The stability of paste fill exposures at the Raleigh Mine was determined by conducting a series of numerical models that incorporate the strength and deformation behaviour of the paste fill, together with the surrounding rock mass response to mining. Stability charts for 2.5 m and 3.5 m wide simultaneous horizontal and vertical exposures have been derived based upon the numerical modelling results.

Due to the increase in modulus and "brittleness" with increasing paste fill strength, an increase in strength beyond a UCS of 275 kPa does not result in an increase in stability.

ACKNOWLEDEMENTS

The authors would like to thank the management of EKJV Management Pty. Ltd. for permission to publish this paper.

The efforts of Celine Bourdeux and Daniel Billaux of Itasca Consultants S.A.S. is also acknowledged.

REFERENCES

AREF, K., HASSANI, F. P. and CHURCHER, D., 1989. A Study on Liquefaction Potential of Paste Backfill. Proceedings of the 4th International Symposium on Mining with Backfill. Montreal, pp. 405-414.

FAIRHURST, C., 1964. On the Validity of the Brazilian Test for Brittle Materials. International Journal of Rock Mechanics and Mineral Sciences., Vol. 1 No.4. pp. 535-546.

MITCHELL, R. J., and WONG, B.C., 1982. Behavior of Cemented Tailings Sands, Canadian Geotechnical Journal, Vol. 19. No.3 pp. 289-295.

NEVILLE, A. M., 1963. Properties of Concrete. London: Pittman.

PAKALNIS, R. CACEERES, C., CLAPP, K., MORIN, M., BRADY, T., WILLIAMS, T., BLAKE, W. and MACLAUGHLIN, M., 2005. Design Spans – Underhand Cut and Fill Mining. CIM-AGM. Toronto.

PIERCE, M., 1997. Laboratory and Numerical Analysis of the Strength and Deformation Behaviour of Paste Backfill. M.Sc. Thesis, Queen’s University, Kingston, Canada.

PIERCE, M., 2000. Stability of Paste Fill Exposures at Brunswick Mine. FLAC and Numerical Modeling in Geomechanics. Balkema, Rotterdam

RANKINE, R. M., RANKINE,K.J., SIVAKUGAN, N., KARUNASENA, W. and BLOSS, M., 2001. Geotechnical Characterisation and Stability Analysis of BHP Cannington Paste Backfill. Proceedings of the 15th ISSMGE Istanbul. pp. 1241-1244.

SAINSBURY, D. P., 2003. An Investigation of the Geomechanical Criteria for Safe and Efficient Crown Pillar Recovery Beneath Cemented Backfill. Ph.D. Thesis, The University of New South Wales, October.

SWAN, G. and BRUMMER, R.K., 2001. Backfill design for deep, Underhand drift-and-fill mining. Minefill 2001: Proceedings of the 7th International Symposium on Mining with Backfill. SME